Impact of GaNAs strain compensation layer on the electronic structure of InAs/GaAs quantum dots*

Song Xin(宋 鑫), Feng Hao(冯 浩), Liu Yu-Min(刘玉敏)†, Yu Zhong-Yuan(俞重远), and Liu Jian-Tao(刘建涛)

State Key Laboratory of Information Photonics and Optical Communications, Beijing University of Posts and Telecommunications, Beijing 100876, *China*

(Received 19 June 2012; revised manuscript received 4 July 2012)

The strain and electron energy levels of InAs/GaAs(001) quantum dots (QDs) with a GaNAs strain compensation layer (SCL) are investigated. The results show that both the hydrostatic and biaxial strain inside the QDs with a GaNAs SCL are reduced compared with those with GaAs capping layers. Moreover, most of the compressive strain in the growth surface is compensated by the tensile strain of the GaNAs SCL, which implies that the influence of the strain environment of underlying QDs upon the next-layer QDs' growth surface is weak and suggests that the homogeneity and density of QDs can be improved. Our results are consistent with the published experimental literature. A GaNAs SCL is shown to influence the strain and band edge. As is known, the strain and the band offset affect the electronic structure, which shows that the SCL is proved to be useful to tailor the emission wavelength of QDs. Our research helps to better understand how the strain compensation technology can be applied to the growth of stacked QDs, which are useful in solar cells and laser devices.

Keywords: strain compensation layer, quantum dots, energy levels, electronic structure

PACS: 73.63.–b, 73.63.Kv, 72.25.Dc, 85.35.Gv **DOI:** 10.1088/1674-1056/22/1/017304

1. Introduction

Recently, self-assembled semiconductor quantum dots (QDs) have attracted intense research interest because of their potential applications in high-efficiency nanostructured solar cells, quantum information processing and optoelectronic devices such as QDs lasers and semiconductor optical amplifiers (SOA).[1–6] Before a large-scale implementation of self-assembled QDs is realized in practical devices some challenging technological issues need to be overcome. Strain is a key factor which not only influences the control and growth of QDs but also affects the QDs' electronic and optical properties. Seeking to improve the absorption efficiency of solar cells and some properties of laser devices, researchers have set higher demands for the density of QDs and multilayer QDs. To increase QDs' density, a stacking technique of QD structures is required just because the active volume of QD structures is smaller than that of the quantum wells (QWs). Though it is known that multi-layer stacking of the QDs by the Stranski–Krastanov (S–K) growth model[7] is a promising way of increasing the overall QD density, typically, stacking of 10 QD layers leads to degradation of the crystal quality and to generation of misfit dislocations as a result of strain accumulation.[8] With the homogeneity of QDs declining and residual strain in QDs systems accumulating, luminous intensity weakens, and inhomogeneous broadening of the QD emissions appears.[9,10]

Recently, strain compensation technology has been applied in research into the preparation of high-quality quantum dot arrays,[11–13] in the hope of solving the problem. Compressive (tensile) strain of QDs is compensated by the tensile (compressive) strain of the compensation layers, so the remaining strain and the thickness of the spacer layer reduce, the homogeneity of QDs is improved, and further, the QDs' optical and electronic characteristics are enhanced.[14]

Through adding the strain compensation layer, seed layer, and strain reduction layer,[15,16] the strain distribution of the QDs system is changed directly or indirectly to improve the size uniformity and density of QDs, which affects intensity and homogeneity of the QDs' emissions. For this reason, tensile-strained barriers such as GaP, GaAsP, and GaNAs have been studied for improving the quality of the QDs' active regions.[17–20] Recently, redshift of emission wavelength, attributed to the strain compensation layer, has also been observed. In these experiments,[17–20] the observation of higher excited states demonstrates that the band filling effect is enhanced with GaNAs SCL, which suggests a smaller contribution of nonradioactive recombination in the QDs sample with GaNAs SCL; the homogeneity and luminescence quantum efficiency are improved with a reduction of average strain in the materials system because the compressive strain is compensated by the tensile strain. Based on the experiments, the electronic structure of InAs/GaAs QDs with GaNAs SCL is investigated by varying the location of the SCL and the thickness of the GaNAs strain compensation layer. The compressive strain in InAs QDs can be released with its expansion by combining with the tensile-strained GaNAs layer, which has a smaller lattice constant than that of GaAs. With the strain compensa-

*Project supported by the National Natural Science Foundation of China (Grant Nos. 60908028, 60971068, 10979065, and 61275201), the Fundamental Research Funds for the Central Universities of Ministry of Education of China (Grant No. 2011RC0402), and the Program for New Century Excellent Talents in University of Ministry of Education of China (Grant No. NCET-10-0261).

†Corresponding author. E-mail: microliuyumin@hotmail.com

© 2013 Chinese Physical Society and IOP Publishing Ltd

tion layer closer to the QDs and the thickness of SCL increasing, the biaxial and hydrostatic strain are compensated more obviously, and the difference of the electron and heavy hole energies is enlarged.

The finite element method of calculating the strain distribution, continuous elastic theory and single band $\boldsymbol{k}\cdot\boldsymbol{p}$ theory are adopted in the work described in this paper. This paper is organized as follows. In Section 2, we present the structure models and theoretical methods used in this work. The strain profiles, the confined energy levels of both electron and heavy hole of QDs embedded GaNAs are shown in Section 3. Finally, the conclusion is drawn.

2. Geometric structure models and theoretical methods

The selection of QDs geometric models is guided by the structures observed in experiment.[21] As shown in Fig. 1, the geometric model is composed of four parts: GaAs substrate, InAs wetting layer, InAs QD and GaNAs SCL. The radius of the bottom is $R = 10$ nm, the radius of the top is $r = 4$ nm, the height is $H = 3$ nm, the thickness of the wetting layer is $w = 0.5$ nm, the height of the $GaN_{0.006}As_{0.994}$ strain compensation layer is h and the distance between the top of the QD and the $GaN_{0.006}As_{0.994}$ SCL is d.

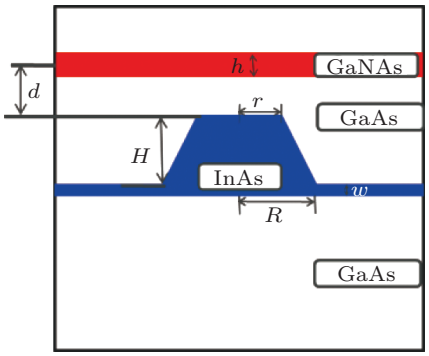


Fig. 1. (color online) Profile of QD with GaNAs SCL model.

In this paper we use the finite element method (FEM) to investigate the strain distributions of self-organized QDs structures based on the continuum elasticity theory.[22,23] The finite element method of calculating the strain distribution has been realized.[17] A comparison has been made between the finite element method and a more accurate atomic method, and the results show that only a little difference can be found near the boundary of the quantum dot.[22,23] The dependence of strain components on stress components can be set up by using a stiffness matrix $\boldsymbol{D}$. For InAs/GaAs as the cubic crystal, the $\boldsymbol{D}$ matrix can be expressed as

$$\boldsymbol{D} = \begin{pmatrix} C_{11} & C_{12} & C_{12} & 0 & 0 & 0 \\ C_{12} & C_{11} & C_{12} & 0 & 0 & 0 \\ C_{12} & C_{12} & C_{11} & 0 & 0 & 0 \\ 0 & 0 & 0 & C_{44} & 0 & 0 \\ 0 & 0 & 0 & 0 & C_{44} & 0 \\ 0 & 0 & 0 & 0 & 0 & C_{44} \end{pmatrix}, \tag{1}$$

and then the stress and the strain may be expressed in terms of two column vectors $\boldsymbol{\sigma}$ and $\boldsymbol{\varepsilon}$

$$\boldsymbol{\sigma} = \begin{pmatrix} \sigma_{xx} \\ \sigma_{yy} \\ \sigma_{zz} \\ \sigma_{xy} \\ \sigma_{yz} \\ \sigma_{xz} \end{pmatrix} = \boldsymbol{D}(\varepsilon - \varepsilon_0) + \sigma_0, \tag{2}$$

$$\varepsilon = \begin{pmatrix} \varepsilon_{xx} \\ \varepsilon_{yy} \\ \varepsilon_{zz} \\ \varepsilon_{xy} \\ \varepsilon_{yz} \\ \varepsilon_{zx} \end{pmatrix} = \begin{pmatrix} \partial u/\partial x \\ \partial v/\partial y \\ \partial w/\partial z \\ (\partial u/\partial x + \partial u/\partial x)/2 \\ (\partial v/\partial z + \partial w/\partial y)/2 \\ (\partial u/\partial z + \partial w/\partial x)/2 \end{pmatrix}, \tag{3}$$

where u, v, and w are the displacements along the coordinates x, y, and z directions respectively; σ_0 is the initial stress and its value is zero; the component of ε_0 is the initial strain in the quantum dot system. In a quantum dot region, the initial strain is the lattice mismatch of the hetero-structure materials. In the surrounding barriers, the initial strain is zero. The lattice mismatch can be expressed as

$$\varepsilon_0 = \frac{\alpha_{\mathrm{InAs}} - \alpha_{\mathrm{GaAs}}}{\alpha_{\mathrm{InAs}}}. \tag{4}$$

The boundary condition is that the bottom side is fixed while other sides are free. The detailed operation steps are shown in Ref. [17].

The electronic structure is calculated in single band envelope approximation with a strain-modified band edge. Based on the strain field, the band offsets are numerically evaluated by the single-band $\boldsymbol{k}\cdot\boldsymbol{p}$ theory. The electron and heavy hole Hamiltonian are[1]

$$H_{\mathrm{e}} = -\frac{\hbar^2}{2m_{\mathrm{e}}^*}\nabla^2 + E_{\mathrm{v,av}} + \frac{\Delta}{3} + E_{\mathrm{g}} + \Delta E_{\mathrm{c}}, \tag{5}$$

$$H_{\mathrm{hh}} = -\frac{\hbar^2}{2m_{\mathrm{hh}}^*}\nabla^2 + E_{\mathrm{v,av}} + \frac{\Delta}{3} + \Delta E_{\mathrm{hh}}, \tag{6}$$

where m_{e}^* is the effective mass tensor of the electron, m_{hh}^* is the effective mass tensor of the heavy hole, $E_{\mathrm{v,av}}$ is the average valence band (VB) energy, Δ is the spin–orbit separation energy, E_{g} is the fundamental gap, ΔE_{c} is the strain modified conduction band edge and ΔE_{hh} is the strain modified heavy hole band edge that can be expressed as

$$\Delta E_{\mathrm{c}} = a_{\mathrm{c}}\varepsilon_{\mathrm{hyd}}, \tag{7}$$

$$\Delta E_{\mathrm{hh}} = a_{\mathrm{v}}\varepsilon_{\mathrm{hyd}} - 0.5b\varepsilon_{\mathrm{bi}}, \tag{8}$$

with a_c, a_v, and b being the deformation potential constants, $\varepsilon_{hyd} = \varepsilon_{xx} + \varepsilon_{yy} + \varepsilon_{zz}$ being the hydrostatic strain and $\varepsilon_{bi} = 2\varepsilon_{zz} - \varepsilon_{xx} - \varepsilon_{yy}$ being the biaxial strain.

The values used in this paper for all kinds of material parameters are given in Table 1.

Table 1. Material parameters.

	GaAs	InAs
Lattice constant α/nm	5.6503	6.0553
Fundamental gap E_g/meV	1518.0	413.0
Averaged VB edge E_V/meV	–6920	–6747
Spin-orbit coupling energy Δ/meV	340	380
Optical matrix parameter E_g/meV	28000	22204
CB effective mass m_e, m_0	0.067	0.022
Luttinger parameter γ_1	7.1	19.7
Luttinger parameter γ_2	2.02	8.4
Luttinger parameter γ_3	2.91	9.3
Kane parameter B/meV·nm^{-2}	0	0
CB hydrostatic def. pot. a_c/meV	–8013	–5080
VB hydrostatic def. pot. a_v/meV	–1160	–1000
VB shear def. pot. b/meV	–2000	–1800
Elastic compliance C_{11}/GPa	118.8	83.8
Elastic compliance C_{12}/GPa	53.8	45.3
Elastic compliance C_{44}/GPa	59.4	39.6

3. Results and discussion

The effects of both the location and the thickness of the strain compensation layer on the strain distribution, conduction band edge and valance band edge are discussed.

In Fig. 2, it is easy to find that inside the QDs with the GaNAs strain compensation layer, the value of the hydrostatic strain decreases and the biaxial strain decreases because both of them are compensated correspondingly. There are abrupt changes in both the hydrostatic strain and the biaxial strain inside the SCL region. However, the influence of the strain compensation outside of QDs is not obvious.

The relations between the thickness and the strain (hydrostatic strain and biaxial strain) distributions are shown in Fig. 3. The thickness of strain compensation layer is 0.5, 1, 1.5, 2, 2.5, 3, 3.5, and 4 nm. With the thickness enhanced, the biaxial strain inside the top of the QDs changes noticeably while that inside the bottom of the QDs changes little. In particular, as illustrated in Fig. 3(b), with a thicker strain compensation layer, the hydrostatic strain inside QDs is compensated more obviously due to more accumulation of strain inside QDs. The values of the hydrostatic and biaxial strain become zero abruptly in the strain compensation layer. As is well known, hydrostatic strain can explain the strain state of materials: the material is tensile when the hydrostatic strain is greater than zero; on the contrary, the material is compressive. Thus, the QD region is tensile and the tensile degree decreases as the strain compensation layer becomes thicker. This can be accounted for in terms of lattice mismatch: N concentration increases as the thickness increases; the ability of lattice strain coordination is enhanced so that the degree of strain relaxation

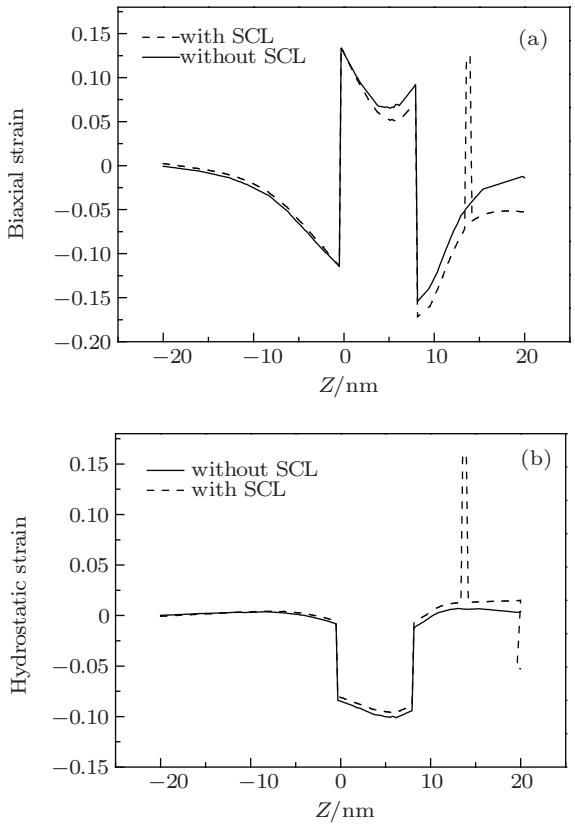


Fig. 2. Comparison of the strain distributions of the QD with $GaN_{0.006}As_{0.994}$ SCL ($d = 3$ nm, $h = 1$ nm) to that without SCL: (a) the biaxial strain distribution; (b) the hydrostatic strain distribution.

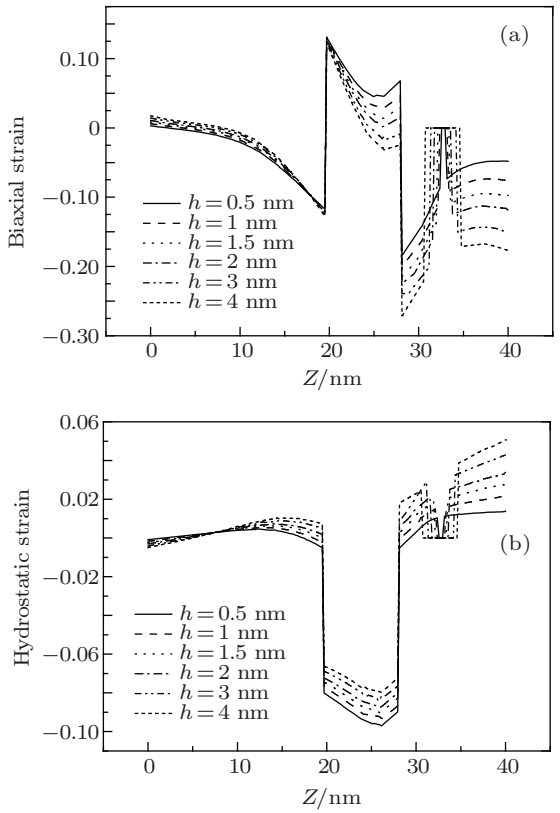


Fig. 3. The strain distributions of QDs with an SCL ($d = 3$ nm). (a) The biaxial strain distribution with different thicknesses of SCL. (b) The hydrostatic strain distribution with different thicknesses of SCL.

in the QDs improves and the compressive strain inside QDs decreases, which leads to more significant compensation.

The result of the strain compensation inside the QDs is related to N density, the thickness and the location of the SCL indirectly.

A comparison of conduction band edge and valance band edge is shown in Fig. 4. From expressions (1) and (2), it can be shown that the band edge modifications are mainly dependent on the hydrostatic strain and biaxial strain components. Affected by the hydrostatic strain, the conduction band edge energy inside QDs with a strain compensation layer decreases while the valance band edge energy increases under influences of the biaxial strain and the hydrostatic strain. Hence, the gap edge of the QD reduces and the emission wavelength of the QD undergoes redshift, which is observed similarly in the experiment.[21]

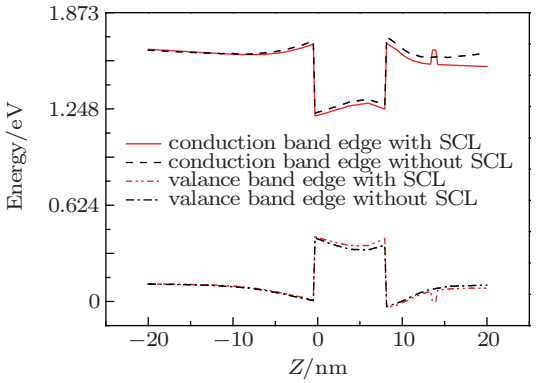


Fig. 4. (color online) Comparison of band edge with $GaN_{0.006}As_{0.994}$ SCL ($d = 3$ nm, $h = 1$ nm) to that without SCL.

Based on Eqs. (6)–(8) we calculate the effects of the conduction band edge and the heavy hole band edge. The relations between the thickness of the SCL and conduction band edge and valance band edge are shown in Fig. 5. As the thickness of SCL increases, the band edge of the region around the SCL is affected more significantly, while there is little influence in the region away from the SCL. The conduction band energy decreases with the value of the hydrostatic strain decrease calculated in Fig. 5(b). Since the value of b is bigger than a_v, the heavy hole band edge is affected by the biaxial strain mostly as seen from Eq. (8). Therefore, with a thicker strain compensation layer, the heavy hole band edge of the QDs' top changes noticeably while that of the QDs' bottom is almost not influenced.

As is calculated, the electron probability densities of the QD without an SCL are the ground state 1.422 eV and excited states 1.522, 1.522, 1.595, 1.601, and 1.609 eV. The electron probability densities of the QD with an SCL are the ground state 1.412 eV and excited states (1.512, 1.512, 1.585, 1.598, and 1.599 eV). From the results, it is deduced that an SCL has little influence on the electron probability density. Because the ground state and the lower excited states are not influenced obviously, only the electron probability densities of the QD with $GaN_{0.006}As_{0.994}$ and that without an SCL are shown in Fig. 6.

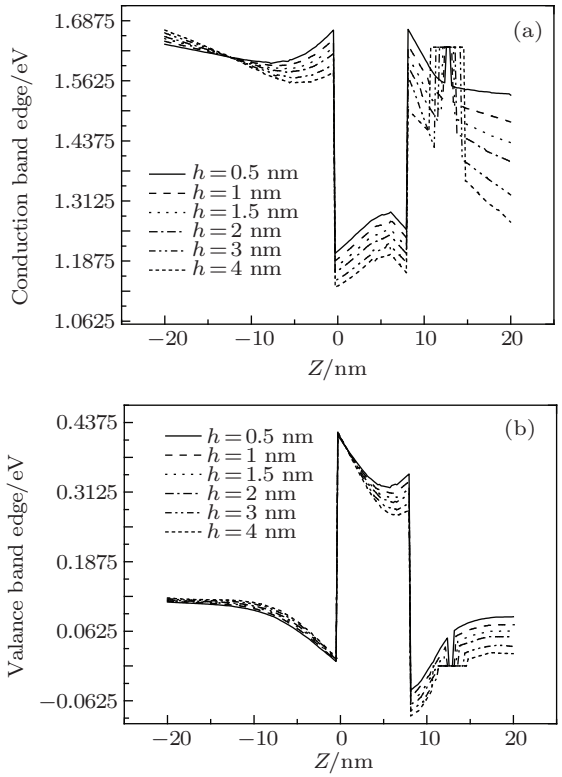


Fig. 5. Band edge of QDs with SCL ($d = 3$ nm). (a) Conduction band edge with different thicknesses of SCL, (b) heavy hole band edge with different thicknesses of SCL.

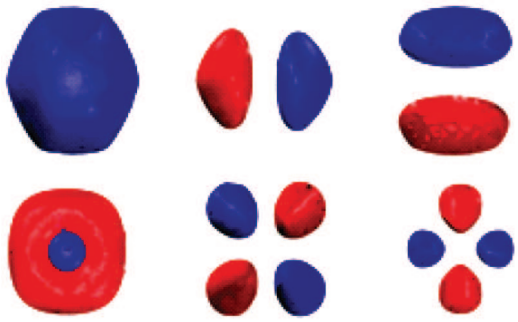


Fig. 6. (color online) The electron probability densities of the QD.

As illustrated in Fig. 7, the carrier energy levels of the QD vary with the location of the SCL changing. The distance d is 3, 4, 5, 6, and 7 nm. When N composition is constant, the electronic ground state gradually increases with the SCL far away from the QD. When the location of the SCL is beyond some range, the SCL will not affect the properties of the QD and the energy levels of the electrons are almost the same as for QDs without an SCL. The variation tendency of the ground state of the heavy hole is similar to that of the electron. However, the carrier energy levels have the same tendency as the N concentration increases. The carrier energy levels with the SCL vary more widely than they do without the SCL. Considering the strain compensation layer, the energy offset of the

QD electronic ground state energy and the heavy hole ground state energy both decrease. Hence, the emission wavelength of QDs will show a redshift with respect to the inter-band transitions of electrons, which improves the optical properties of GaNAs-embedded QD, as has been explained based on past experiments.[24]

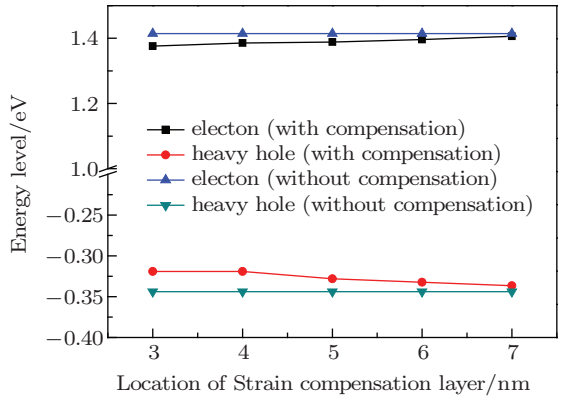


Fig. 7. (color online) The relations between the ground state of carrier energy levels and the location of the SCL ($h = 1$ nm).

In Fig. 8, the ground state of electrons decreases while that of the heavy holes increases with the thickness of the SCL increasing. With a thicker SCL, the lattice coordinates better, so the accumulated strain decreases. The energy difference of the electron and hole ground state decreases as the SCL thickness increases, so the emission wavelength of QDs will show a redshift.

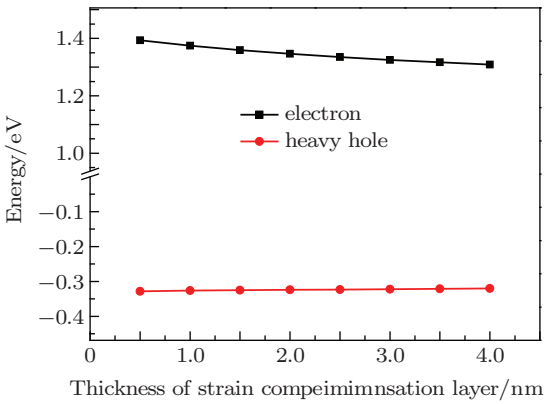


Fig. 8. (color online) The relation between the ground state of carrier energy levels and the thickness of SCL.

4. Conclusion

In this work, we gain some interesting and meaningful conclusions as summarized below by investigating the strain, electron energy levels and optical properties of an InAs/GaAs(001) quantum dot with GaNAs SCL.

(i) The strain distribution and the confinement energy levels of the QD with GaNAs SCL and without SCL are discussed. With the strain compensation layer, since GaNAs has a smaller lattice constant than that of GaAs, the compressive strain in the InAs QD is partly compensated by the tensile strain of the strained GaNAs layer, so the electron energy levels decrease while the hole energy levels increase, which results in redshift of the emission wavelength.

(ii) The location of the SCL also influences the carrier energy levels. With the SCL closer to the QD, the compensated result is more obvious and the ground state energy differences of the electrons and holes decrease, which enhances the redshift of the emission wavelength.

(iii) With the thickness of the SCL increasing (i.e. with N density increasing), strain relaxation is enhanced, so the strain accumulation inside QDs decreases and then the electron and heavy hole band edge are influenced, which illustrates that the electronic and optical properties of QDs can be better with a thicker SCL.

All of our simulation results are in accord with published experimental findings.[9] The research of the strain compensation layer is based on the growing quality (homogenization and volume density) of QDs array. The varying behavior of the carrier energy levels with changes in strain compensation provides a new approach for tuning QD photoluminescence properties.

References

[1] Arakawa Y and Sakaki H 2002 *Appl. Phys. Lett.* **40** 939
[2] Padiha L A, Neves A R, Rodriguez E, Cesar C L, Barbosa L C and Brito Cruz C H 2005 *Appl. Phys. Lett.* **86** 161111
[3] Sugawara M, Ebe H, Hatori N and Ishida M 2004 *Phys. Rev.* B **69** 35332
[4] Oshima R, Takata A and Shoji Y 2010 *Physica* E **42** 2757
[5] Takata A, Ayami, Okada Y and Yoshitaka O 2001 *Appl. Phys. Lett.* **93** 083111
[6] Hubbard S M, Cress C D, Bailey C G, Raffaelle R P, Bailey S G and Wilt D M 2008 *Appl. Phys. Lett.* **92** 123512
[7] Oshima R, Hashimoto T, Shigekawa H and Okada Y 2006 *J. Appl. Phys.* **100** 083110
[8] Tersoff J, Teichert C and Lagally M G 1996 *Phys. Rev. Lett.* **76** 1675
[9] Wasilewski Z R, Fafard S and McCaffrey J P 1999 *J. Cryst. Growth* **201** 1131
[10] Wang X D, Liu N, Shih C K, Govindaraju S and Holmes A L 2004 *Appl. Phys. Lett.* **85** 1356
[11] Oshima R, Nakamura Y, Takata A and Okada Y 2008 *J. Cryst. Growth* **310** 2234
[12] Oshima R, Takata A and Okada Y 2008 *Appl. Phys. Lett.* **93** 083111
[13] Nuntawong N, Xin Y C, Birudavolu S, Huang P S, Hains C P and Huffaker D L 2005 *Appl. Phys. Lett.* **86** 193115
[14] Ganapathy S, Zhang X Q, Uesugi K, Kumano H and Suemune I 2002 *IEEE 18th International Semiconductor Laser Conference* September 29–October 3, 2002 Garmisch-Partenkirchen, Germany, pp. 151,152
[15] Nabetani Y and Matsumoto T 2005 *J. Appl. Phys.* **98** 063502
[16] Tatebayashi J, Nuntawong N, Wong P S, Xin Y C, Lester L F and Huffaker D L 2009 *J. Phys.* D: *Appl. Phys.* **42** 073002
[17] Liu Y M, Yu Z Y and Ren X M 2008 *Chin. Phys. Lett.* **25** 1850
[18] Takata A, Oshima R, Shoji Y and Okada Y 2009 *J. Crys. Growth* **311** 1774
[19] Lin C H, Pai W W, Chang F Y and Lin H H 2007 *Appl. Phys. Lett.* **90** 063102
[20] Akahane K, Yamamoto N, Gozu S, Ueta A and Ohtani N 2006 *Physica* E **32** 81
[21] Nagarajan S, Aierken A and Jussila H 2011 *Semicond. Sci. Technol.* **26** 1242
[22] Liu Y M, Yu Z Y and Ren X M 2008 *Chin. Phys. Lett.* **25** 1850
[23] Liu Y M, Yu Z Y and Ren X M 2009 *Chin. Phys.* B **18** 1056
[24] Oshima R, Nakamura Y, Takata A and Okada Y 2008 *J. Crys. Growth* **310** 2234